THE JOURNAL OF BIOLOGICAL CHEMISTRY VOL. 286, NO. 20, pp. 18026–18036, May 20, 2011

A Multi-domain Fragment of Nogo-A Protein Is a Potent Inhibitor of Cortical Axon Regeneration via Nogo Receptor 1*[S]

Received for publication, November 30, 2010, and in revised form, March 9, 2011 Published, JBC Papers in Press, March 24, 2011, DOI 10.1074/jbc.M110.208108

Eric A. Huebner[‡], Byung G. Kim[‡§], Philip J. Duffy[‡], Rebecca H. Brown[‡], and Stephen M. Strittmatter[‡1]

From the [‡]Department of Neurology and Program in Cellular Neuroscience, Neurodegeneration, and Repair, Yale University School of Medicine, New Haven, Connecticut 06536 and the [§]Brain Disease Research Center, Institute for Medical Sciences, and Department of Neurology, Ajou University School of Medicine, Suwon 443-749, Korea

Nogo-A limits axon regeneration and functional recovery after central nervous system injury in adult mammals. Three regions of Nogo-A (Nogo-A-24, Nogo-66, and Nogo-C39) interact with the neuronal Nogo-66 receptor 1 (NgR1). Nogo-66 also interacts with a structurally unrelated cell surface receptor, paired immunoglobulin-like receptor (PirB). We show here that the other two NgR1-interacting domains, Nogo-A-24 and Nogo-C39, also bind to PirB with high affinity. A purified 22-kDa protein containing all three NgR1- and PirB-interacting domains (Nogo-22) is a substantially more potent growth cone-collapsing molecule than Nogo-66 for chick dorsal root ganglion neurons and mature cortical neurons. Moreover, Nogo-22 inhibits axon regeneration of mature cortical neurons *in vitro* more potently than does Nogo-66. Although all three NgR1-interacting domains of Nogo-A also interact with PirB, expression of PirB in mature cortical cultures is nearly undetectable. Consistent with a relatively minor role for PirB in mature cortical neurons, Nogo-22 inhibition of axon regeneration is abolished by genetic deletion of NgR1. Thus, NgR1 is the predominant receptor for Nogo-22 in regenerating cortical neurons.

Axonal sprouting and long-distance regeneration are restricted by numerous inhibitory molecules within the mature, injured mammalian CNS (1). Axon growth inhibitors include the myelin-associated inhibitors and the chondroitin sulfate proteoglycans.

The most well characterized myelin-associated inhibitor is Nogo-A. The importance of Nogo-A in limiting axonal growth *in vivo* has been demonstrated. For example, antibodies targeting Nogo-A promote axon regeneration and enhance functional recovery after CNS injury (2, 3). Additionally, an NgR1[2] antagonist peptide (NEP1–40), which competitively interferes with the Nogo-66 portion of Nogo-A binding to NgR1, promotes corticospinal tract (CST) axon regeneration and functional recovery after spinal cord injury (4, 5). Genetic deletion of Nogo-A has yielded conflicting results. Although some studies fail to detect an effect of Nogo deletion (6, 7), other studies report enhanced axonal sprouting, long-distance axon regeneration, and functional recovery after spinal cord injury (SCI) in Nogo-deficient mice (8, 9). Potential reasons for this discrepancy include differences in mouse age, background strain, and details of the gene disruption (10). However, even in *Nogo-ab*$^{atg/atg}$ mice, in which significant long-distance CST regeneration is not detected, enhanced CST sprouting after unilateral pyramidotomy occurs (11). Thus, Nogo-A clearly restricts axonal growth within the injured CNS.

Two regions of Nogo-A have been shown to inhibit axon growth. One of these, Amino-Nogo, acts by an NgR1-independent mechanism to disrupt integrin function (12). A second region, Nogo-66, interacts with NgR1 to limit axon growth (13) (Fig. 2*A*). Two additional regions (Nogo-A-24 and Nogo-C39), separated from Nogo-66 by transmembrane domains, also interact with NgR1 (14, 15) (Fig. 2*A*). By themselves, Nogo-A-24 and Nogo-C39 have not been shown to activate NgR1 to cause axonal growth inhibition or RhoA activation. However, a fragment of Nogo-A containing the Nogo-A-24 sequence (Y4C) fused directly to Nogo-66 creates a ligand with substantially higher affinity for NgR1-transfected COS-7 cells than either segment alone (14). Moreover, Nogo-A-24 fused to the first 32 amino acids of Nogo-66 creates a more potent inhibitor of embryonic chick DRG neurite outgrowth compared with Nogo-66 alone (14). However, both of these fusion ligands lack the intervening transmembrane domain that normally separates Nogo-A-24 and Nogo-66 and thus may not precisely mimic the physiological Nogo-A/NgR1 interaction. In addition, initial attempts to produce sufficient quantities of Nogo-A-24:Nogo-66 fusion protein to test in neurite outgrowth assays were unsuccessful. We show here that a 22-kDa portion of Nogo-A that contains all three NgR1-interacting domains and includes the endogenous transmembrane domains (Nogo-22) is a substantially more inhibitory ligand than Nogo-66 alone.

PirB was identified as a second receptor capable of binding to Nogo-66 and mediating at least part of its inhibitory activity in certain neuronal types (16). Comparisons of the relative roles, redundancy, and function of NgR1 *versus* PirB have been partial and incomplete. In acute, high-potency collapse assays, both proteins appear to be required for Nogo-66 function in sensory neurons (16, 17). Chronic outgrowth assays have utilized dehydrated and potentially denatured myelin or Nogo-66 at much

* This work was supported, in whole or in part, by National Institutes of Health Grants MSTP TG T32GM07205 (to E. A. H.) and R01NS42304, R01NS39962, and R01NS33020 (to S. M. S.). This work was also supported by the Falk Medical Research Trust (to S. M. S.). S. M. S. is a cofounder of Axerion Therapeutics, which seeks to develop PrP- and NgR-based therapeutics.

[S] The on-line version of this article (available at http://www.jbc.org) contains supplemental Fig. S1.

[1] To whom correspondence should be addressed. E-mail: stephen.strittmatter@yale.edu.

[2] The abbreviations used are: NgR1, Nogo-66 receptor 1; CST, corticospinal tract; DRG, dorsal root ganglion; PirB, paired immunoglobulin-like receptor; E13, embryonic day 13; DIV, day(s) *in vitro*; AP, alkaline phosphatase.

higher concentrations and have never studied mature cerebral cortical neurons, which are relevant for a greater number of neurological injuries. Here, we extend the assessment of NgR1 *versus* PirB and show that Nogo-A-24 and Nogo-C39 also bind to PirB with high affinity, suggesting that PirB could mediate inhibitory signaling by Nogo-22 as completely as NgR1. However, PirB expression in mature cortical cultures is nearly undetectable, suggesting a relatively minor role for PirB in cortical neurons. By direct testing with soluble, high-potency Nogo-22, we find that Nogo inhibition of axon regeneration in cortical cultures is abolished by genetic deletion of NgR1. Thus, Nogo-22 is a potent inhibitor of axon regeneration and signals through NgR1 in mature cortical neurons.

EXPERIMENTAL PROCEDURES

COS-7 Cell Binding Assay—The COS-7 cell binding assay has been described previously (14, 15). COS-7 cells were transfected with plasmids encoding mouse NgR1 or PirB.

Nogo-22 kDa Protein Production and Purification—Production of the Nogo-22 kDa protein, containing residues 950–1192 of mature human Nogo-A, has been described previously (18). Following elution from the GST column, Nogo-22 was dialyzed extensively against 50 mM Tris (pH 7.4), 100 mM NaCl, 1 mM DTT, and 1 mM EDTA at 4° using Slide-A-Lyzer dialysis cassettes (10K MWCO) (Thermo Scientific). The final dialysis was against Neurobasal A (Invitrogen). Following dialysis, the solution was ultracentrifuged at 100,000 × *g* for 1 h to remove insoluble material. The supernatant was filtered through a 0.2-μm filter to sterilize it. Protein concentration was determined using a Quick Start Bradford protein assay (Bio-Rad). Aliquots were stored at −80° C until use. The vehicle control consisted of 3 mM lauryldimethylamine N-oxide dialyzed against the same reservoir of 50 mM Tris-HCl (pH 7.4), 100 mM NaCl, 1 mM DTT, and 1 mM EDTA as the matching Nogo-22 preparation. For protein size and purity analysis, dialyzed Nogo-22 was separated by SDS-PAGE, and the gel was stained with Coomassie Brilliant Blue.

Size Exclusion Chromatography—Purified Nogo-22 protein (2 mg) in 200 μl of 50 mM Tris-HCl (pH 7.4), 100 mM NaCl, and 3 mM lauryldimethylamine *N*-oxide was chromatographed through a 24-ml Superdex 200 column equilibrated in the same buffer. Absorbance at 256 nm was monitored using an ÄKTA purifier system (GE Healthcare).

E13 Chick DRG Growth Cone Collapse Assay—The chick DRG growth cone collapse assay has been described previously (19, 20).

Mouse DRG Neurite Outgrowth Assay—The adult mouse DRG neurite outgrowth assay has been described previously (18). Wells were coated with 60 ng/cm^2 of Nogo-22. Data from 12–15 wells (four to five wells in three separate DRG preparations) were collected.

Immunoblots—Cortical cultures were established as for the cortical axon regeneration assay (see below) and cultured for 2 h (0 weeks *in vitro*) to 4 weeks. Cultures were rinsed twice on ice with cold PBS and then lysed with 50 mM Tris-HCl (pH 7.4), 150 mM NaCl, 1% Triton X-100, 0.1% SDS, 1% sodium deoxycholate, plus protease inhibitors (Roche) (lysis buffer). Cell lysates were sonicated and then centrifuged at 14,000 × *g* for 30 min. Proteins were separated by SDS-PAGE and transferred to a PVDF membrane. For brain and spleen samples, tissue was obtained from adult (3 months or older) mice, homogenized in lysis buffer using a ground glass homogenizer, and then processed as for cortical cultures. NgR$^{-/-}$ brain (Fig. 4*A*) and PirB$^{-/-}$ brain and spleen (Fig. 4, *B* and *C*) were used as negative controls. PirB$^{-/-}$ mice were kindly provided by Marc Rothenberg (Cincinnati Children's Hospital Medical Center, Cincinnati, OH) (21, 22). The following primary antibodies were used: goat anti-NgR (R&D Systems, AF1440, 1:1,000), goat anti-PirB (R&D Systems, AF2754, 1:400), rabbit anti-GAPDH (Santa Cruz Biotechnology, sc-25778, 1:1,000), and mouse anti-actin (Sigma-Aldrich, 1:2,000). Appropriate IRDye 680CW and 800CW secondary antibodies were used (Li-Cor Biosciences, 1:5,000). Blots were visualized and signals quantitated using the Odyssey infrared imaging system (Li-Cor Biosciences).

Cortical Axon Regeneration Assay (Cortical Scrape Assay)—Primary cortical cultures were established from E18 Sprague-Dawley rat embryos (Charles River Laboratories). All tissue culture reagents were from Invitrogen unless stated otherwise. Brains were dissected in Hibernate E without calcium (BrainBits LLC) supplemented with B-27, 1 mM sodium pyruvate, and 10 μg/ml gentamicin (dissection medium). Reagents and brains were kept on ice except for the brain being dissected. Meninges were removed, and cortices were dissected and combined in a 10-cm Petri dish in 1 ml of dissection medium. Cortices were diced ~100 times into small pieces with a razor blade. 12 ml of dissection medium plus 4.2 mg/ml papain (Sigma-Aldrich, P4762) and 0.8 mg/ml DNase were added to the Petri dish, which was then placed on an orbital shaker (Fisher, 11–671-50Q) in a 37° C incubator (without CO_2 regulation). The dish was shaken gently (30 rpm) for 1 h. The dish was removed from the incubator, and the medium was transferred to a 15-ml polystyrene Falcon tube on ice. Chunks of cortex were allowed to settle to the bottom of the tube for 1–2 min. The medium was removed, and chunks were resuspended in 1.5 ml of dissection medium plus 10% FBS and triturated 10–15 times with a fire-polished Pasteur pipette. The medium, containing dissociated cortices, was transferred to another 15-ml tube containing 12.5 ml of dissection medium plus 10% FBS and centrifuged at 600 × *g* for 6 min at 4° C. The supernatant was removed, and cells were resuspended in 12 ml of Neurobasal A supplemented with B-27, 1 mM sodium pyruvate, 0.5 mM GlutaMAX-I, and 10 μg/ml gentamicin (Neurobasal A plus supplements). Cells were filtered through a 70-μm cell strainer into a 50-ml Falcon tube and counted. Cells were removed from ice and diluted to 3.33 × 10^5 cells/ml in Neurobasal A plus supplements, which had been prewarmed and preequilibrated in a 37° C tissue culture incubator (5% CO_2). Cells were plated at a density of 1.2 × 10^5 cells/cm^2 (4 × 10^4 cells/well in 120 μl) in 96-well poly-D-lysine-coated plates (BD Biosciences). Door openings over the ensuing 26 days were minimized. At 7 and 14 DIV, cultures were fed by replacing 50% of the medium with fresh, prewarmed, and preequilibrated Neurobasal A plus supplements.

At 21 DIV, cultures were injured by scraping with a 96-well floating pin tool with FP1-WP pins (V&P Scientific). To guide the movement of the pin tool, a library copier (V&P Scientific, VP 381NW4.5) with vertical alignment holes was used. Alumi-

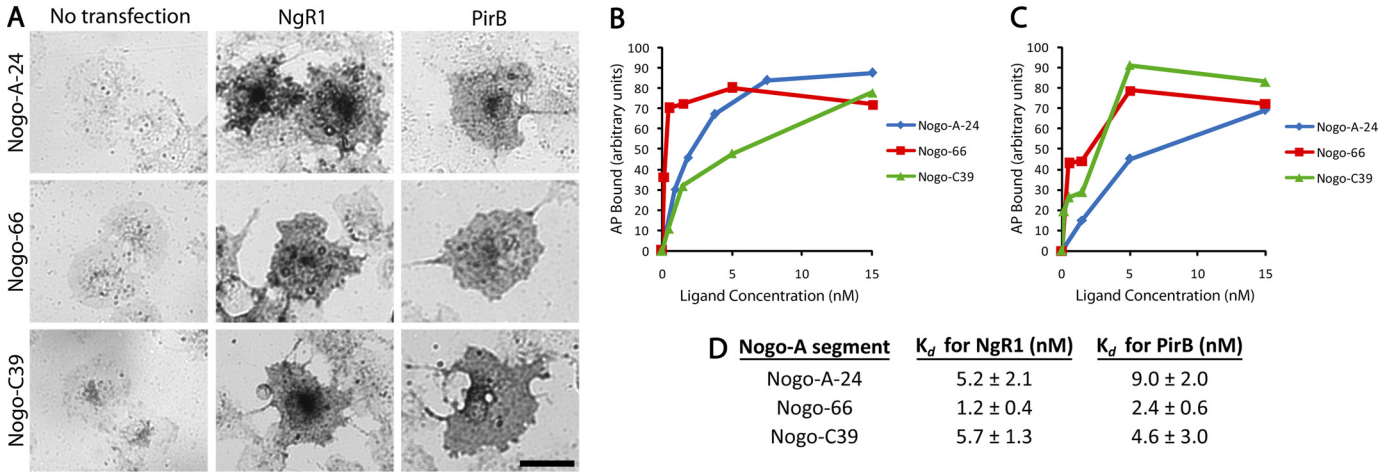

D

Nogo-A segment	K_d for NgR1 (nM)	K_d for PirB (nM)
Nogo-A-24	5.2 ± 2.1	9.0 ± 2.0
Nogo-66	1.2 ± 0.4	2.4 ± 0.6
Nogo-C39	5.7 ± 1.3	4.6 ± 3.0

FIGURE 1. **Three domains of Nogo-A bind to NgR1 and to PirB.** *A*, COS-7 cell binding assay showing that Nogo-A-24, Nogo-66, and Nogo-C39 (all 15 nM) bind to NgR1- or PirB-transfected COS-7 cells. No binding to non-transfected COS-7 cells is detected. *B* and *C*, ligand binding as a function of concentration to NgR1-transfected (*B*) or PirB-transfected (*C*) COS-7 cells. One representative binding curve for each ligand-receptor interaction is shown. The experiment was repeated three times with similar results. *D*, K_d values for ligand interactions with NgR1 and PirB are reported. Data are mean ± S.E. from three independent determinations. *Scale bar* = 50 μm.

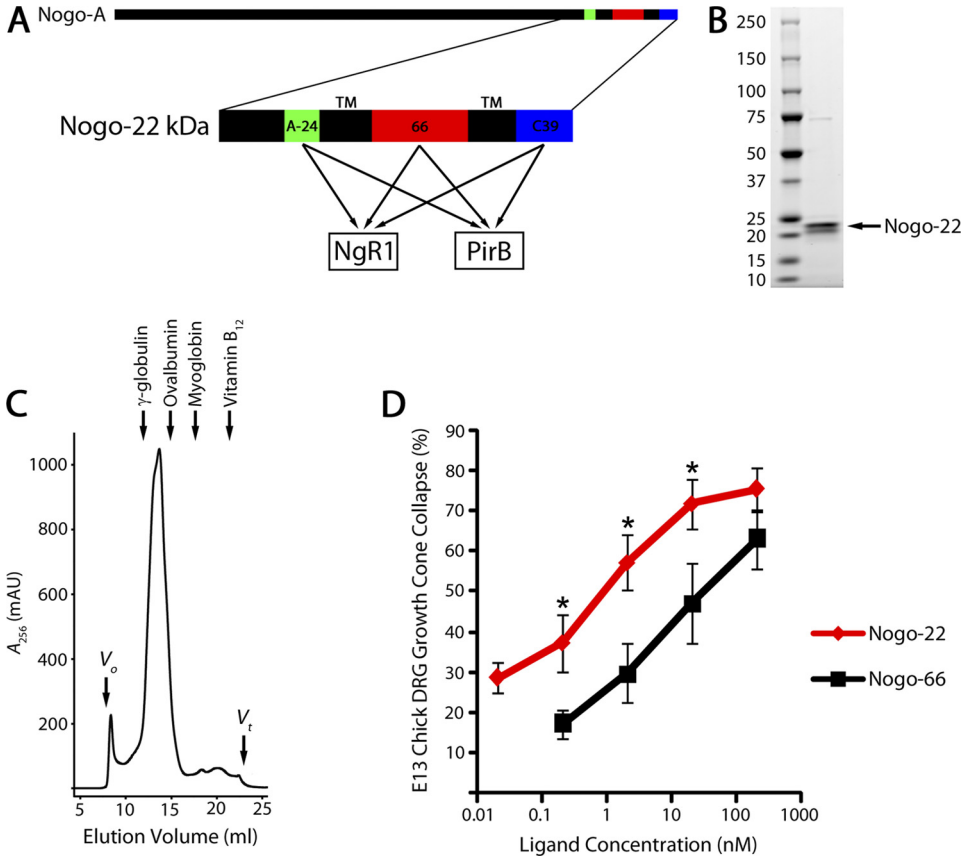

FIGURE 2. **Nogo-22 kDa is a potent inhibitory region of Nogo-A.** *A*, schematic of the human Nogo-A protein illustrating the 22-kDa C-terminal region which contains three NgR1- and PirB-interacting domains. *B*, Coomassie-stained SDS-PAGE gel showing that purified Nogo-22 kDa migrates as two bands near the expected 22-kDa size. *C*, size exclusion chromatography of purified Nogo-22 reveals a major peak corresponding to a molecular weight of ~80 kDa. Approximate elution positions for protein standards are indicated. *D*, E13 chick DRG growth cone collapse assay showing that Nogo-22 is a >10-fold more potent growth cone-collapsing molecule than Nogo-66. *A-24*, Nogo-A-24; *66*, Nogo-66; *C39*, Nogo-C39; V_o, void volume; V_t, total volume.

num guide rails were added on the left and right of the library copier (Electronic and Machine Shop, Yale University School of Medicine) to minimize lateral movement of the pin tool. Immediately after the scrape, 50% of the medium was replaced with fresh medium. In some cases, the fresh medium contained soluble inhibitor and/or drug(s). Cultures were returned to the incubator to regenerate for 5 days.

At 26 DIV, cultures were fixed by adding 100 μl/well of 4% paraformaldehyde plus 20% sucrose in PBS for 20 min, blocked/permeabilized with 10% normal goat serum plus 0.1% Triton

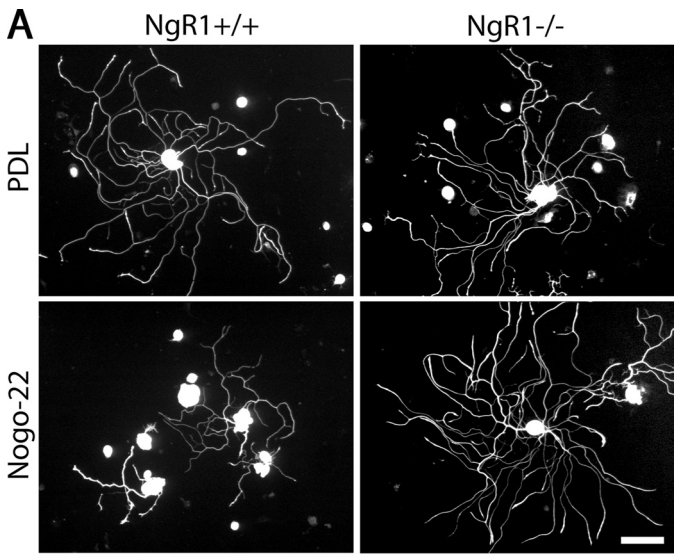

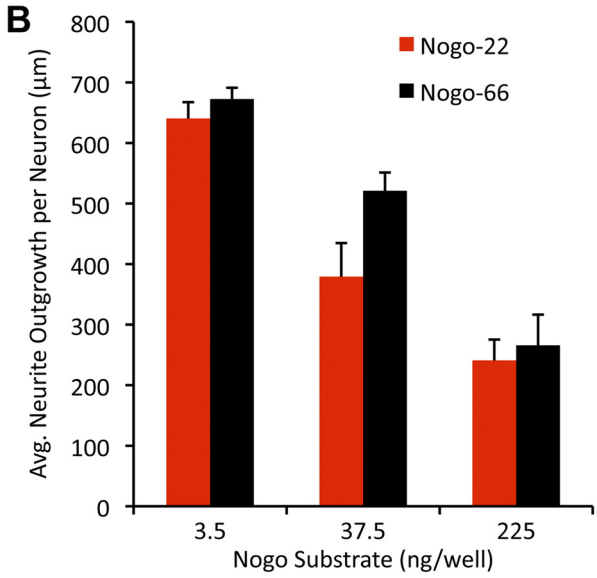

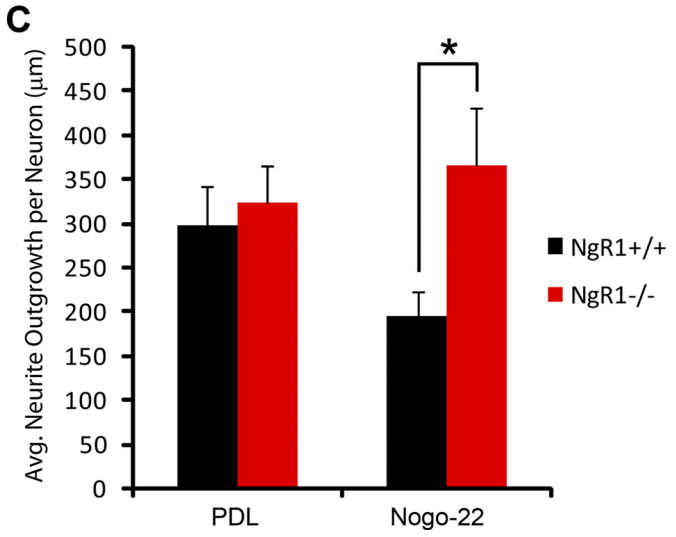

FIGURE 3. **NgR-dependence of Nogo-22 inhibition.** *A*, photomicrographs of dissociated adult DRG neurons (NgR1$^{+/+}$ and NgR1$^{-/-}$) cultured for 18 h on control or Nogo-22 substrates and immunostained for βIII-tubulin. *B*, measurement of neurite outgrowth from NgR1$^{+/+}$ neurons on substrates coated with different amounts of Nogo-66 or Nogo22, as indicated. Data are mean ± S.E. $n = 4$. *C*, quantification of neurite outgrowth shows significantly more outgrowth for NgR1$^{-/-}$ neurons cultured on Nogo-22 compared with NgR1$^{+/+}$ neurons. Data are mean ± S.E. $n = 12–15$. *, $p < 0.05$, Student's two-tailed *t* test. *Scale bar* = 100 μm. *PDL*, poly-D-lysine.

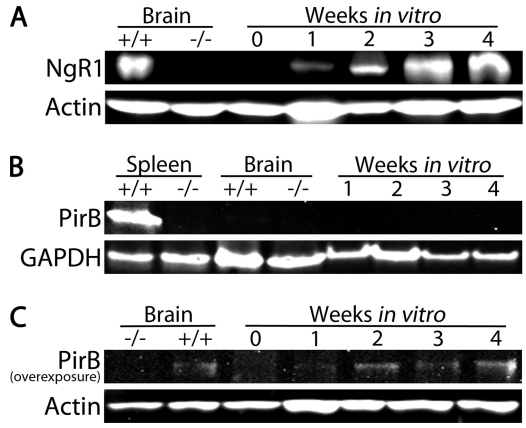

FIGURE 4. **NgR1 and PirB expression in cortical cultures.** *A*, immunoblot showing a time course for NgR1 expression in cortical cultures isolated from the E18 cortex. Immediately after isolation (0 weeks *in vitro*), NgR1 expression is nearly undetectable. NgR1 expression increases with time in culture and by 3 to 4 weeks *in vitro* is similar to that in the adult WT brain. Adult *NgR1*$^{-/-}$ brain was used as a negative control, and actin was used as a loading control. *B*, immunoblot showing that PirB is not readily detected in the adult WT brain or in cortical cultures. Adult WT spleen was used as a positive control, and GAPDH was used as a loading control. *C*, overexposure of a Western blot for PirB reveals that PirB is faintly detected in the adult WT brain and in cortical cultures.

X-100 in PBS for 30 min, and immunostained for βIII-tubulin (Promega, G7121, 1:1,000). An Alexa Fluor 488 goat anti-mouse IgG secondary antibody was used (Invitrogen, A11029, 1:500). Images were acquired with an ImageXpress Micro imaging system (Molecular Devices) using a 10× objective. Axon regeneration was analyzed using MetaXpress Version 1.7 software. The center (~75%) of the lesion was analyzed by cropping the image and analyzing axon growth using an angiotube formation algorithm. The area covered by axons was measured, and all values were normalized to the control. Typically, data from 12–36 wells (4–12 wells from three separate cortical preparations) were collected.

Mouse cortical cultures do not regenerate as well as rat cortical cultures at 21 DIV, but they do regenerate well at 7 DIV. Therefore, for the *NgR1*$^{-/-}$ *versus* *NgR1*$^{+/+}$ scrape assay experiment (Fig. 9) and MAP2 immunohistology (Fig. 5, *D–F*), in which mouse cultures were used (C57BL/6, Charles River Laboratories), scrapes were done at 7 DIV. For MAP2 immunohistology, an anti-MAP2 antibody (Cell Signaling Technology, #4542, 1:50) was used.

Cortical Growth Cone Collapse Assay—The same protocol used for the cortical axon regeneration assay was followed, except that at 26 DIV (5 days post-scrape), 10 μl of medium containing vehicle or soluble inhibitor was added to each well to induce growth cone collapse. Cultures were returned to the incubator for 30 min and then fixed and immunostained as for the cortical axon regeneration assay, except that rhodamine phalloidin (Invitrogen, R415, 1:100) was also included with the secondary antibody to visualize F-actin-rich growth cones. The average area per growth cone and the number of growth cones were deter-

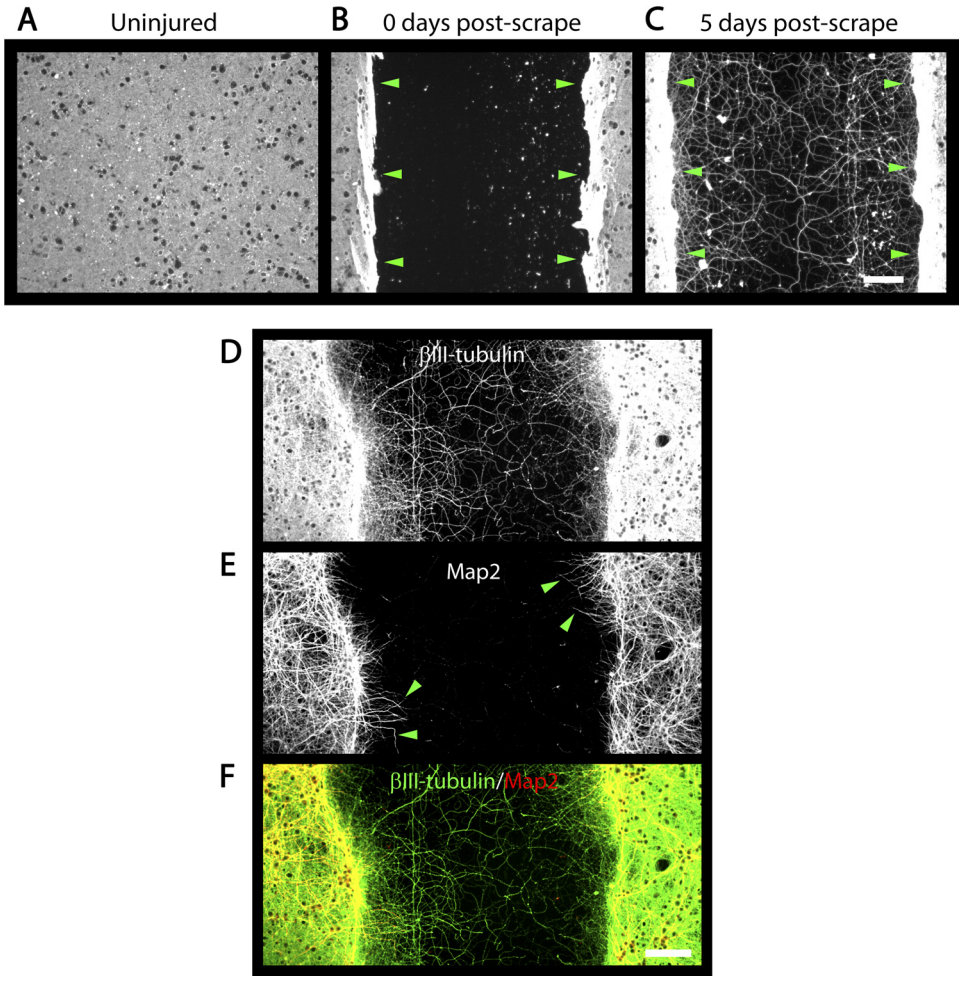

FIGURE 5. **Cortical axon regeneration assay.** *A–C*, photomicrographs of cortical cultures immunostained for βIII-tubulin. *A*, uninjured 21 DIV cultures have a dense network of neurites covering the well bottom. *B*, immediately after a scrape injury at 21 DIV, a region in the well center is devoid of neurites and cell bodies. *C*, 5 days after a scrape injury, βIII-tubulin-positive neurites have regenerated into the lesion. *Green arrowheads* indicate the edges of the lesion (*B* and *C*). Regenerated neurites throughout the lesion are immunoreactive for βIII-tubulin (*D*), whereas MAP2-immunoreactivity (*E*) is restricted to neurites near the edges of the lesion (*green arrowheads*) and the dense network of neurites outside of the lesion. *F*, merged image showing that MAP2 (*red*) colocalizes with a subset of βIII-tubulin-positive neurites (*green*). *Scale bars* = 100 μm.

mined using ImageJ software. To calculate the growth cone index, the average area per growth cone was multiplied by the number of growth cones per mm^2 of axon for individual wells, and then growth cone index values for multiple wells were averaged.

RESULTS

Three Domains of Nogo-A Bind to NgR1 and to PirB—Three regions near the C terminus of Nogo-A (Nogo-A-24, Nogo-66, and Nogo-C39) have been shown previously to interact with NgR1 (14, 15). One of these domains, Nogo-66, also interacts with PirB (16). To determine whether the other two NgR1-interacting domains (Nogo-A-24 and Nogo-C39) also interact with PirB, we tested alkaline phosphatase (AP) fusion ligands in a COS-7 cell binding assay (Fig. 1). All three AP-tagged ligands bind to NgR1-transfected COS-7 cells with dissociation constants (K_d) in the low nanomolar range, confirming previous results (14, 15). AP-Nogo-66 binds to PirB-transfected COS-7 cells, confirming a previous report (16). Importantly, the other two NgR1-interacting ligands, AP-Nogo-A-24 and AP-Nogo-C39, also bind to PirB-transfected COS-7 cells with K_d in the low nanomolar range (9.0 ± 2.0 and 4.6 ± 3.0 nM, respectively). These results demonstrate that all three known NgR1-interacting domains of Nogo-A also bind to PirB with low nanomolar affinities.

Nogo-22 kDa Is a Potent Inhibitory Region of Nogo-A—The most physiologically relevant reagent would contain all three NgR1- and PirB-interacting domains separated by the endogenous transmembrane domains. We developed a method to produce and purify this ligand (18). Because this protein is 22 kDa in length, it has been termed Nogo-22 kDa or Nogo-22 (Fig. 2*A*). Purified Nogo-22, detected by SDS-PAGE and Coomassie staining, appears as two bands near the expected 22-kDa size (Fig. 2*B*), presumably representing alternative tobacco etch virus cleavage during purification. Size exclusion chromatography of purified Nogo-22, in the presence of lauryldimethylamine *N*-oxide, reveals a major peak corresponding to a molecular weight of ~80 kDa (Fig. 2*C*). These data are consistent with Nogo-22 forming a homotrimer or homotetramer.

The inhibitory activity of Nogo-22, after detergent removal by dialysis, was tested and compared with that of Nogo-66 using purified ligands in a standard DRG growth cone collapse assay. Nogo-22 induces collapse of E13 chick DRG growth cones

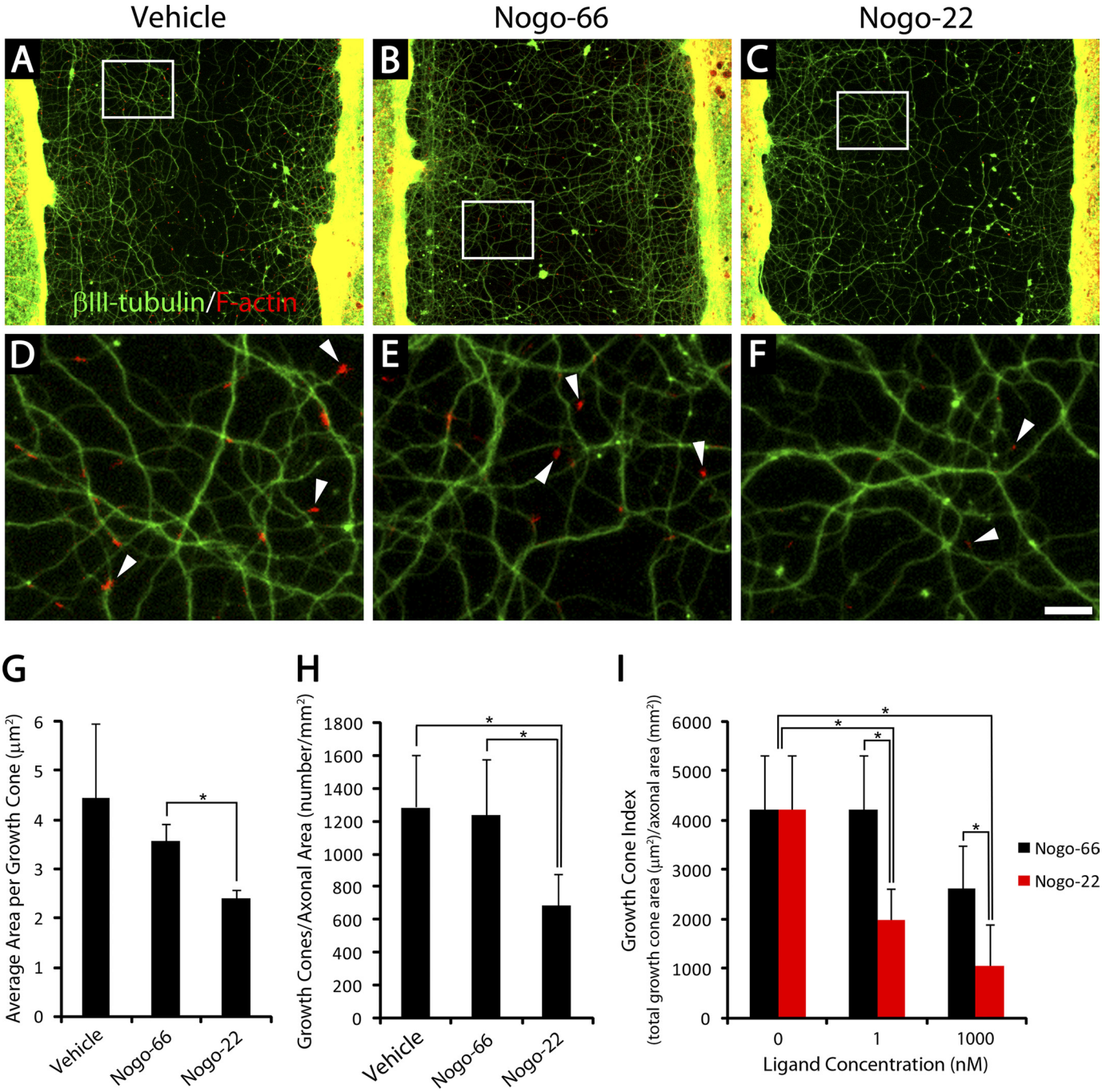

FIGURE 6. **Nogo-22 induces collapse of cortical growth cones.** *A–F*, photomicrographs of cortical cultures that were scraped at 21 DIV and regenerated for 5 days in the presence of vehicle (*A* and *D*), Nogo-66 (*B* and *E*), or Nogo-22 (*C* and *F*). Phalloidin staining reveals F-actin-rich growth cones (*red*) at the tips of regenerating βIII-tubulin-positive neurites (*green*). *D–F*, higher magnification of boxed regions in *A–C*. *White arrowheads* indicate growth cones. *G*, quantification of the average area per growth cone in cultures treated with vehicle, 1 nM Nogo-66, or 1 nM Nogo-22. Cultures treated with Nogo-22 have significantly smaller growth cones on average than cultures treated with Nogo-66. *H*, quantification of the number of growth cones visible, normalized to axonal area. Cultures treated with 1 nM Nogo-22 have significantly fewer growth cones visible than cultures treated with 1 nM Nogo-66 or vehicle. *I*, a simplified measure of total growth cone area (growth cone index, see text for details) demonstrates that Nogo-22 is a more potent growth cone-collapsing agent than Nogo-66 at two ligand concentrations. Data are mean ± S.E. $n = 15$. *Scale bar* = 100 μm (*A–C*), 19 μm (*D–F*). *, $p < 0.05$, Student's two-tailed *t* test.

with >10-fold greater potency compared with Nogo-66. This result indicates that Nogo-22 is a more potent growth cone-collapsing molecule than Nogo-66 for embryonic chick DRG neurons and is consistent with the notion that Nogo-22 is a higher-affinity NgR1 agonist than Nogo-66.

The role of NgR1 in Nogo-22 inhibition was examined using dissociated DRG cultures from adult *NgR1*$^{+/+}$ (wild-type) or *NgR1*$^{-/-}$ mice (23). Cells were cultured for 18 h on control substrate or immobilized Nogo-22 (Fig. 3). In the substrate-bound assay, as in the soluble ligand collapse assay, Nogo-22 is inhibitory at lower doses than Nogo-66 (Fig. 3*B*). No difference in neurite outgrowth between *NgR1*$^{+/+}$ or *NgR1*$^{-/-}$ neurons is observed on control substrate. However, *NgR1*$^{-/-}$ neurons display significantly

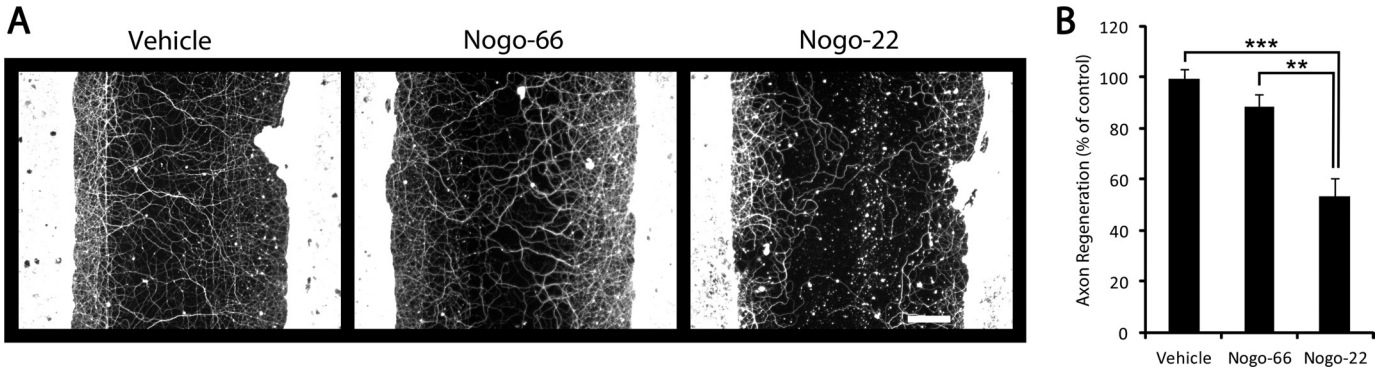

FIGURE 7. **Nogo-22 inhibits mature cortical axon regeneration.** *A*, photomicrographs of cortical cultures that were scraped at 21 DIV and regenerated for 5 days. βIII-tubulin immunostaining allows visualization of regenerated axons. Vehicle, Nogo-66, or Nogo-22 (620 nM) were included soluble in the media during the 5-day regeneration period. *B*, quantification of axon regeneration illustrates that Nogo-22 significantly inhibits axon regeneration relative to Nogo-66 or vehicle. Data are mean ± S.E. $n = 12–27$. *Scale bar* = 100 μm. **, $p < 0.01$; ***, $p < 0.001$; Student's two-tailed *t* test.

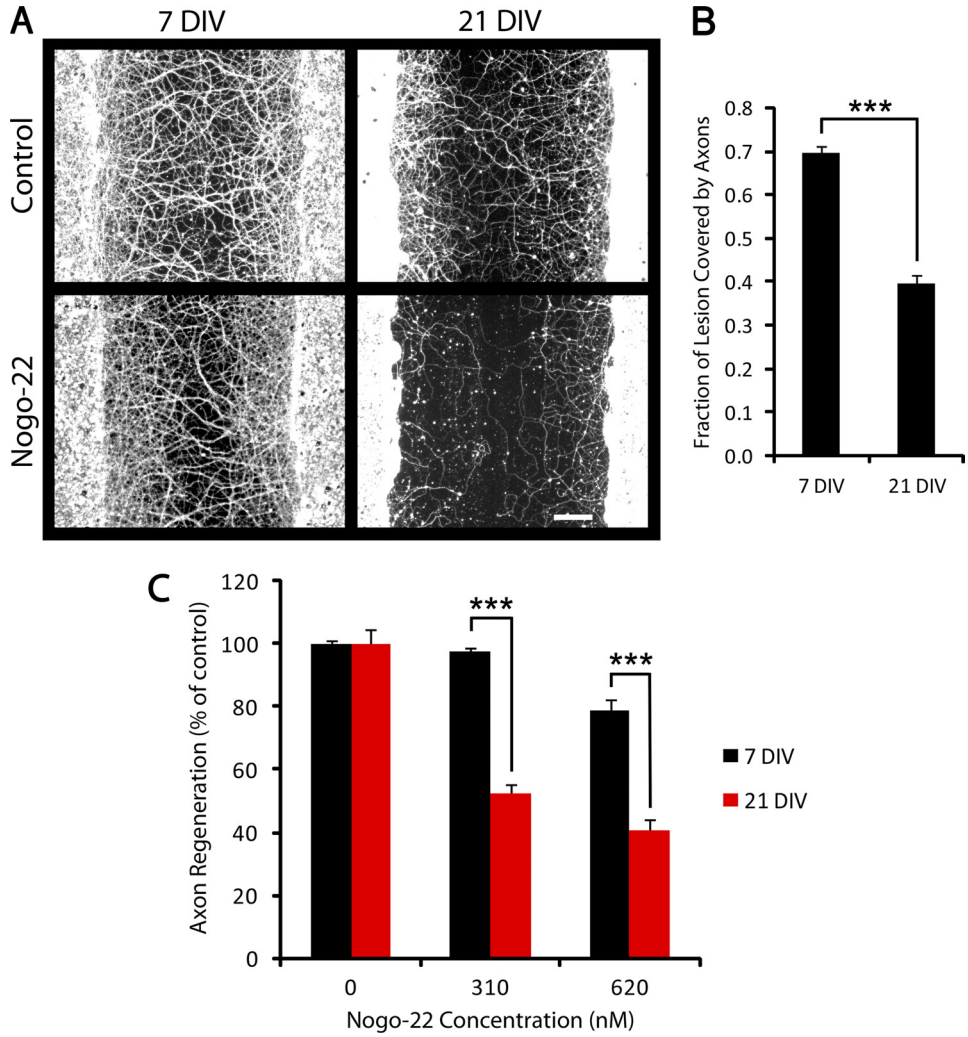

FIGURE 8. **21 DIV cortical cultures are more sensitive than 7 DIV cultures to Nogo-22 inhibition.** *A*, βIII-tubulin immunostaining of cortical cultures that were scraped at 7 or 21 DIV and regenerated for 5 days in the absence or presence of Nogo-22 (310 nM). *B*, quantification of axon regeneration in the absence of inhibitor (control condition), indicating that cultures scraped at 7 DIV regenerate more than cultures scraped at 21 DIV. *C*, quantification of axon regeneration relative to control in the presence of Nogo-22. Axon regeneration in cultures scraped at 7 DIV is modestly inhibited by the higher concentration of Nogo-22 but is not inhibited by the lower concentration. In contrast, axon regeneration in cultures scraped at 21 DIV is significantly inhibited by both concentrations of Nogo-22, indicating greater sensitivity to Nogo-22 for 21 DIV cultures. Data are mean ± S.E. $n = 33–42$. *Scale bar* = 100 μm. ***, $p < 0.001$, Student's two-tailed *t* test.

more neurite outgrowth than $NgR1^{+/+}$ neurons on Nogo-22 (Fig. 3, *A* and *C*), implicating NgR1 as a functional receptor for Nogo-22 in adult mouse DRG neurons.

Nogo-22 Induces Growth Cone Collapse in Mature Cortical Neurons—To study Nogo-22 inhibition in a cell type relevant to stroke, traumatic brain injury, and spinal cord injury, we cul-

tured cortical neurons from the rodent cerebral cortex. However, at embryonic or early postnatal stages, when these neurons are most readily isolated, they express little or no NgR1 (24). By postnatal day 15, NgR1 is readily detected in the cerebral cortex (24). Cultures established from the E18 cortex show a similar expression pattern, with nearly undetectable levels present immediately after isolation and an increase in NgR1 expression with time in culture (Fig. 4*A*). By 3 to 4 weeks *in vitro*, NgR1 expression is similar to that in the adult brain (Fig. 4*A*).

PirB expression is nearly undetectable in the adult WT brain or in cortical cultures by immunoblotting, although it is readily detected in the spleen (Fig. 4*B*). With a relatively long blot exposure time, PirB is faintly detected in WT brain and in cortical cultures, with 2 to 4 week *in vitro* cultures having the highest, albeit still low, expression (Fig. 4*C*).

Based primarily on the NgR1 expression pattern, we sought to study Nogo-22 inhibition in 21 DIV cortical cultures. Cortical cultures were scraped with a custom multi-pin tool at 21 DIV to create reproducible axonal injury. Prior to injury, a dense network of βIII-tubulin-positive neurites is present (Fig. 5*A*). Immediately after scrape injury, the lesion center is devoid of neurites (Fig. 5*B*). During the ensuing 5 days, neurite regeneration into the lesion occurs (Fig. 5*C*).

The majority of regenerated neurites within the lesion center are MAP2-negative (Fig. 5, *D–F*), suggesting axonal rather than dendritic identity. A few MAP2-positive fibers are seen near the lesion edges, suggesting that some dendritic growth occurs for a short distance into the lesion (Fig. 5, *E* and *F*).

Double staining for F-actin and βIII-tubulin reveals F-actin-rich growth cones at the tips of neurites within the lesion (Fig. 6, *A* and *D*), suggesting that regeneration is still occurring at 5 days post-injury when the cultures are fixed.

Growth cone collapse can be induced by adding soluble inhibitor to the media 5 days after scrape injury and 30 min prior to fixation (Fig. 6). 1 nM Nogo-22 significantly decreases the average area per growth cone compared with 1 nM Nogo-66 (Fig. 6*G*). In addition, the number of growth cones visible (normalized to axonal area) is significantly reduced by 1 nM Nogo-22, but not by 1 nM Nogo-66, compared with vehicle control (Fig. 6*H*). A simplified measure of total growth cone area (growth cone index = average area per growth cone × number of growth cones visible, normalized to axonal area) (Fig. 6*I*) illustrates that Nogo-22 is a more potent growth cone-collapsing agent than Nogo-66 at two different concentrations. These data indicate that Nogo-22 is a more potent growth cone-collapsing agent than Nogo-66 in mature, regenerating cortical neurons.

Nogo-22 Inhibits Axon Regeneration of Mature Cortical Neurons—Inhibition of long-distance axon regeneration contributes substantially to the persistence of functional deficits after spinal cord and brain injury. Therefore, we investigated the potential for Nogo-22 to inhibit axon regeneration in injured cortical cultures when included soluble in the media for the entire 5-day regeneration period (Fig. 7). An automated method for quantification of axon regeneration in the lesion center was employed (supplemental Fig. S1). Nogo-22 significantly inhibits axon regeneration relative to Nogo-66 or vehicle

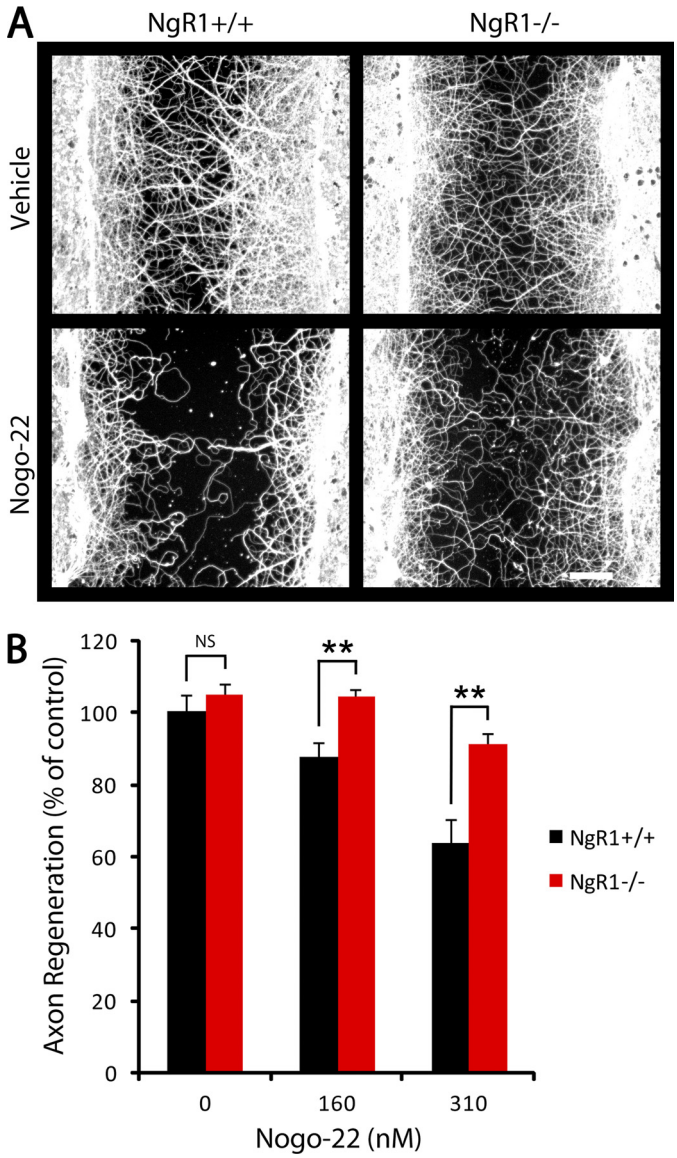

FIGURE 9. **Nogo-22 inhibition of cortical axon regeneration is NgR-dependent.** *A*, βIII-tubulin immunostaining of NgR1$^{+/+}$ and NgR1$^{-/-}$ cortical cultures that were scraped and regenerated for 5 days in the presence of vehicle or Nogo-22. *B*, quantification of axon regeneration. No difference in axon regeneration in the absence of inhibitor is detected between the two genotypes. Significantly more axon regeneration is present in NgR1$^{-/-}$ cultures in the presence of both concentrations of Nogo-22 compared with NgR1$^{+/+}$ cultures. Data are mean ± S.E. $n = 9–12$. *Scale bar* = 100 μm. **, $p < 0.01$, Student's two-tailed *t* test. *NS*, not significant.

control (Fig. 7*B*). Thus, Nogo-22 is a more potent inhibitor than Nogo-66 of axon regeneration in mature cortical neurons.

Nogo-22 Inhibition of Cortical Neuron Axon Regeneration Is NgR1-dependent—Because NgR1 expression increases with time in culture, we hypothesized that older cultures are more sensitive to Nogo-22 than are younger cultures. To test this prediction, 7 DIV and 21 DIV cultures were scraped and allowed to regenerate for 5 days in the absence or presence of Nogo-22. The fraction of the lesion covered by axons in the absence of inhibitor (control condition) is greater for cultures scraped at 7 DIV than for cultures scraped at 21 DIV (Fig. 8*B*), indicating more regeneration in younger cultures. However, to examine sensitivity to Nogo-22 in terms of % inhibition, the

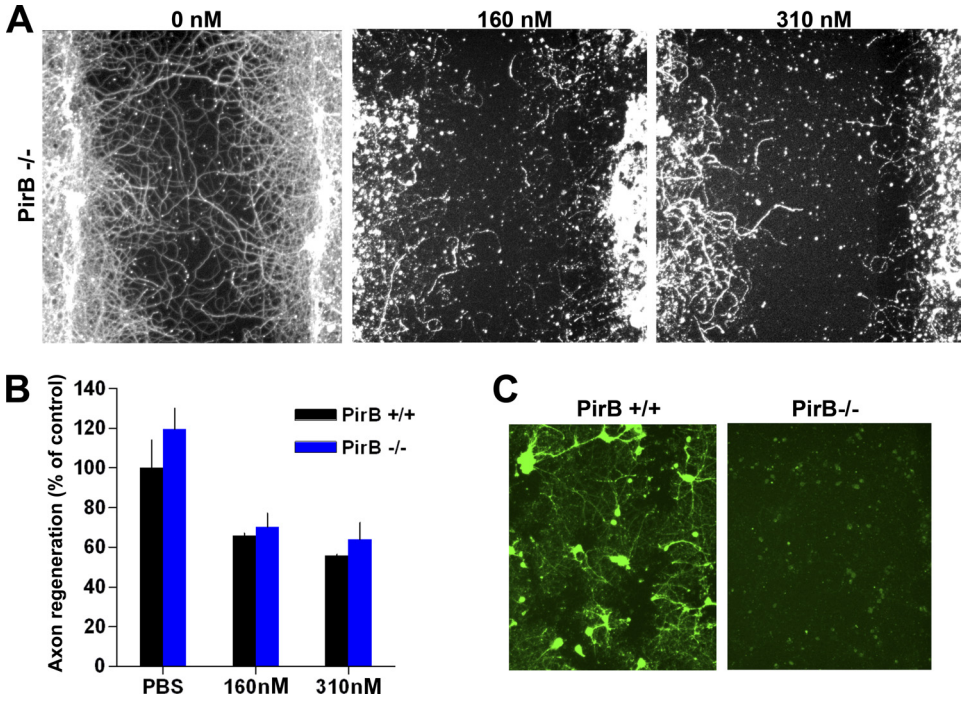

FIGURE 10. **PirB is not required for Nogo-22 inhibition of cortical axon regeneration.** *A*, βIII-tubulin immunostaining of PirB$^{+/+}$ cortical cultures that were scraped and regenerated for 5 days in the presence of vehicle or Nogo-22 at the indicated concentrations. *B*, quantification of axon regeneration. No difference in axon regeneration in the presence or absence of Nogo-22 is detected between the two genotypes. Data are mean ± S.E. $n = 4–5$ cultures from separate mice. *C*, anti-PirB immunohistology from WT or PirB$^{-/-}$ cultures at 5 days after a scrape injury and within 400 μm of the scrape border. A genotype-specific immunohistological signal is detected in the vicinity of the scrape.

control was assigned a value of 100% for both 7 DIV and 21 DIV cultures (Fig. 8*C*). As predicted, axon regeneration in 21 DIV cultures is inhibited significantly more at a given concentration of Nogo-22 than in 7 DIV cultures. A slight effect of Nogo-22 on the number of DAPI-positive nuclei present in the intact area of the culture adjacent to the scrape occurs (data not shown). However, normalizing regeneration to nuclear number does not substantially affect the results (data not shown). These results correlate with the time course of NgR1 expression in cortical cultures (Fig. 4*A*) and suggest that NgR1 could mediate Nogo-22 inhibition in mature cortical neurons.

To unambiguously demonstrate a role for NgR1 in Nogo-22-mediated inhibition of axon regeneration in cortical neurons, we tested *NgR1*$^{+/+}$ and *NgR1*$^{-/-}$ cultures (Fig. 9). No difference in regeneration in the absence of inhibitor is observed between the two genotypes. Axon regeneration is inhibited by Nogo-22 in *NgR1*$^{+/+}$ cultures in a dose-dependent manner. Inhibition of axon regeneration is significantly attenuated in *NgR1*$^{-/-}$ cultures, compared with *NgR1*$^{+/+}$ cultures, in the presence of 160 and 310 nM Nogo-22. Axon regeneration in *NgR1*$^{-/-}$ cultures at both concentrations of Nogo-22 is not significantly different from the WT control. These results indicate that NgR1 is the predominant receptor for Nogo-22 in mature cortical neurons and suggest a relatively minor or non-existent role for PirB.

To directly test the role of PirB, we performed similar experiments with PirB$^{-/-}$ neurons (Fig. 10). While there is some detectable expression of PirB protein adjacent to scrape injuries detected immunohistologically (Fig. 10*C*), the inhibitory effect of Nogo-22 is not reduced by deletion of PirB (Fig. 10, *A* and *B*) as compared with NgR1 (Fig. 9).

The ROCK Inhibitor Y27632 Attenuates Nogo-22 Inhibition of Axon Regeneration—Nogo-66 binding to NgR1 activates the kinase ROCKII, leading to inhibition of axon growth (25). The ROCKII inhibitor Y27632 promotes neurite growth in the presence of inhibitory substrates and promotes axon regeneration and recovery of function after spinal cord injury (26). To investigate the potential requirement of ROCKII for Nogo-22-mediated inhibition of axon regeneration, we tested Y27632 for its ability to overcome Nogo-22 inhibition in the cortical axon regeneration assay (Fig. 11). Y27632 does not significantly affect regeneration in the absence of the inhibitor. However, Y27632 significantly attenuates inhibition by Nogo-22, restoring regeneration to a level indistinguishable from control conditions (Fig. 11*B*). This suggests that ROCKII is required for Nogo-22-mediated inhibition of axon regeneration in mature cortical neurons.

DISCUSSION

This study extends our understanding of the mechanisms by which Nogo-A limits axon regeneration. We show that all three known NgR1-interacting domains of Nogo-A (Nogo-A-24, Nogo-66, and Nogo-C39) bind to PirB with low nanomolar affinities. Additionally, we characterize a 22-kDa fragment of Nogo-A that contains all three NgR1 and PirB-interacting domains (Nogo-22). We find that Nogo-22 is a more potent growth cone-collapsing agent and a more potent inhibitor of axon regeneration than Nogo-66. For technical reasons, we were unable to directly determine a K_d for Nogo-22/NgR1 or Nogo-22/PirB interactions. However, results presented here, taken together with previous findings (14), suggest that the K_d for the Nogo-22/NgR1 interaction is likely to be at least 10-fold

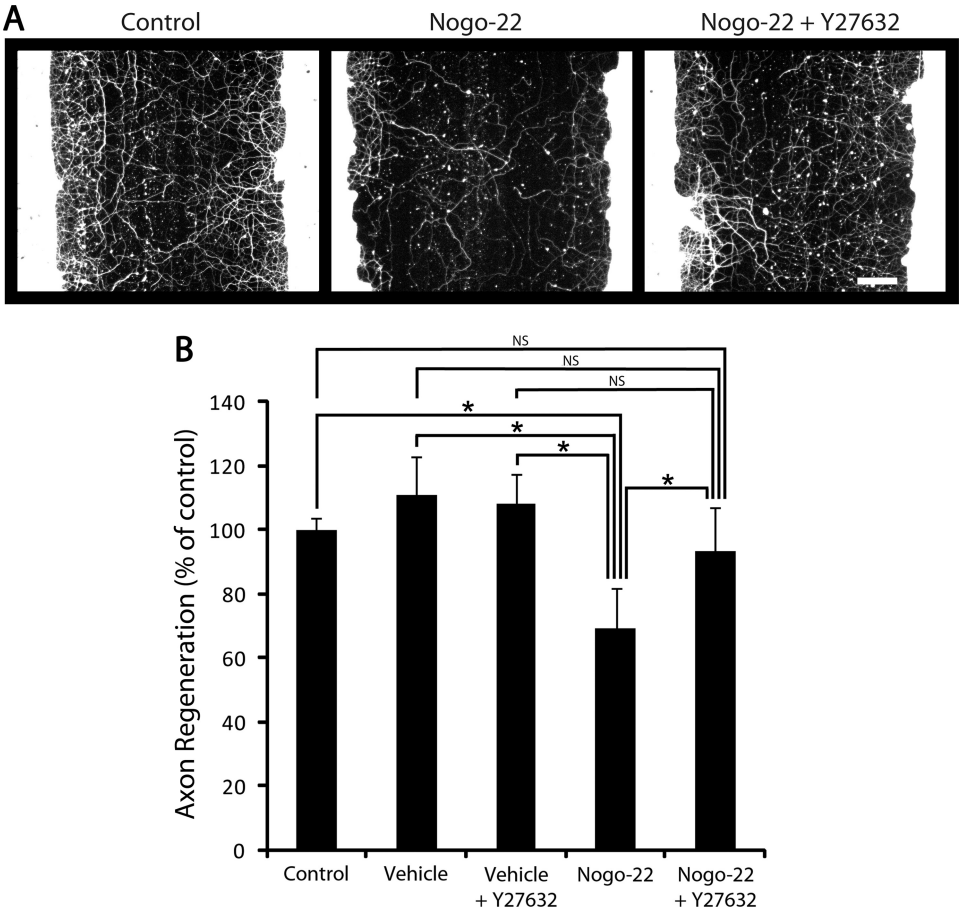

FIGURE 11. **The ROCK inhibitor Y27632 overcomes Nogo-22 inhibition of cortical axon regeneration.** *A*, photomicrographs of mature cortical cultures immunostained for βIII-tubulin 5 days after a scrape injury. In some wells, Nogo-22 (310 nM) and/or Y27632 (25 μM) were included in the media during the regeneration period. *B*, quantification of axon regeneration. Nogo-22 inhibition of axon regeneration is significantly alleviated by Y27632. Data are mean ± S.E. $n = 12$. *Scale bar* = 100 μm. *, $p < 0.05$, Student's two-tailed *t* test. *NS*, not significant.

lower than the K_d for the Nogo-66/NgR1 interaction. This prediction is based on the following observations: 1) A fragment of Nogo-A that contains Nogo-A-24 (Y4C) fused to Nogo-66 creates a ligand with an approximately 10-fold higher affinity than either segment alone (14). Adding the third NgR1-interacting domain, Nogo-C39, might enhance this affinity further. 2) Nogo-22 is a >10-fold more potent growth cone-collapsing agent than Nogo-66 (this study).

Because PirB is nearly undetectable in cortical cultures and Nogo-22 inhibition is abolished by genetic deletion of NgR1, we conclude that NgR1 is the most important receptor for Nogo-22 in mature cortical neurons. Similarly, in our adult mouse DRG neurite outgrowth assay, Nogo-22 inhibition requires NgR1. However, it is possible that PirB plays a significant role in axon growth inhibition in other neuronal types and culture conditions. Indeed, Atwal *et al.* (16) demonstrate that PirB appears to play a role in Nogo-66 and myelin inhibition of cerebellar granule neurons and DRGs and in myelin-associated glycoprotein (MAG) and oligodendrocyte myelin glycoprotein (OMgp) inhibition of cerebellar granule neurons (16). It will be interesting to assess the contribution of PirB to axon growth inhibition in other neuronal types, such as retinal ganglion neurons, both *in vitro* and *in vivo*.

The low levels of PirB protein expression in cortical cultures and in adult brain are consistent with a recent report indicating that CST or rubrospinal sprouting into the denervated spinal cord is not enhanced in $PirB^{-/-}$ mice after unilateral traumatic brain injury (27). Moreover, CST regeneration is not enhanced in $PirB^{-/-}$ mice after dorsal hemisection spinal cord injury (28). These findings do not support a central role for PirB in limiting axon regeneration after cortical neuronal injury. However, it is possible that a redundant role for PirB in cortical neuron axon regeneration failure might be revealed in NgR1/PirB double-knockout mice.

We conclude that the full-length Nogo-22 kDa portion of Nogo-A is a potent inhibitor of axon regeneration and that NgR1 is the predominant receptor for Nogo-22 in mature cortical neurons.

REFERENCES

1. Huebner, E. A., and Strittmatter, S. M. (2009) in *Cell Biology of the Axon* (Koenig, E. ed) pp. 339–351, Springer, Berlin
2. Liebscher, T., Schnell, L., Schnell, D., Scholl, J., Schneider, R., Gullo, M., Fouad, K., Mir, A., Rausch, M., Kindler, D., Hamers, F. P., and Schwab, M. E. (2005) *Ann. Neurol.* **58,** 706–719
3. Seymour, A. B., Andrews, E. M., Tsai, S. Y., Markus, T. M., Bollnow, M. R., Brenneman, M. M., O'Brien, T. E., Castro, A. J., Schwab, M. E., and Kartje, G. L. (2005) *J. Cereb. Blood Flow Metab.* **25,** 1366–1375
4. GrandPré, T., Li, S., and Strittmatter, S. M. (2002) *Nature* **417,** 547–551
5. Li, S., and Strittmatter, S. M. (2003) *J. Neurosci.* **23,** 4219–4227
6. Zheng, B., Ho, C., Li, S., Keirstead, H., Steward, O., and Tessier-Lavigne, M. (2003) *Neuron* **38,** 213–224

7. Lee, J. K., Geoffroy, C. G., Chan, A. F., Tolentino, K. E., Crawford, M. J., Leal, M. A., Kang, B., and Zheng, B. (2010) *Neuron* **66,** 663–670
8. Kim, J. E., Li, S., GrandPré, T., Qiu, D., and Strittmatter, S. M. (2003) *Neuron* **38,** 187–199
9. Cafferty, W. B., Duffy, P., Huebner, E., and Strittmatter, S. M. (2010) *J. Neurosci.* **30,** 6825–6837
10. Cafferty, W. B., Kim, J. E., Lee, J. K., and Strittmatter, S. M. (2007) *Neuron* **54,** 195–199
11. Cafferty, W. B., and Strittmatter, S. M. (2006) *J. Neurosci.* **26,** 12242–12250
12. Hu, F., and Strittmatter, S. M. (2008) *J. Neurosci.* **28,** 1262–1269
13. Fournier, A. E., GrandPre, T., and Strittmatter, S. M. (2001) *Nature* **409,** 341–346
14. Hu, F., Liu, B. P., Budel, S., Liao, J., Chin, J., Fournier, A., and Strittmatter, S. M. (2005) *J. Neurosci.* **25,** 5298–5304
15. Laurén, J., Hu, F., Chin, J., Liao, J., Airaksinen, M. S., and Strittmatter, S. M. (2007) *J. Biol. Chem.* **282,** 5715–5725
16. Atwal, J. K., Pinkston-Gosse, J., Syken, J., Stawicki, S., Wu, Y., Shatz, C., and Tessier-Lavigne, M. (2008) *Science* **322,** 967–970
17. Chivatakarn, O., Kaneko, S., He, Z., Tessier-Lavigne, M., and Giger, R. J. (2007) *J. Neurosci.* **27,** 7117–7124
18. Duffy, P., Schmandke, A., Schmandke, A., Sigworth, J., Narumiya, S., Cafferty, W. B., and Strittmatter, S. M. (2009) *J. Neurosci.* **29,** 15266–15276
19. Liu, B. P., Fournier, A., GrandPré, T., and Strittmatter, S. M. (2002) *Science* **297,** 1190–1193
20. Takahashi, T., Fournier, A., Nakamura, F., Wang, L. H., Murakami, Y., Kalb, R. G., Fujisawa, H., and Strittmatter, S. M. (1999) *Cell* **99,** 59–69
21. Uehara, T., Bléry, M., Kang, D. W., Chen, C. C., Ho, L. H., Gartland, G. L., Liu, F. T., Vivier, E., Cooper, M. D., and Kubagawa, H. (2001) *J. Clin. Invest.* **108,** 1041–1050
22. Munitz, A., McBride, M. L., Bernstein, J. S., and Rothenberg, M. E. (2008) *Blood* **111,** 5694–5703
23. Kim, J. E., Liu, B. P., Park, J. H., and Strittmatter, S. M. (2004) *Neuron* **44,** 439–451
24. Wang, X., Chun, S. J., Treloar, H., Vartanian, T., Greer, C. A., and Strittmatter, S. M. (2002) *J. Neurosci.* **22,** 5505–5515
25. Niederöst, B., Oertle, T., Fritsche, J., McKinney, R. A., and Bandtlow, C. E. (2002) *J. Neurosci.* **22,** 10368–10376
26. Fournier, A. E., Takizawa, B. T., and Strittmatter, S. M. (2003) *J. Neurosci.* **23,** 1416–1423
27. Omoto, S., Ueno, M., Mochio, S., Takai, T., and Yamashita, T. (2010) *J. Neurosci.* **30,** 13045–13052
28. Nakamura, Y., Fujita, Y., Ueno, M., Takai, T., and Yamashita, T. (2011) *J. Biol. Chem.* **286,** 1876–1883